Combination of Palbociclib and Erlotinib Exhibits Synergistic Antitumor Effect in Colorectal Cancer Patient-Derived Xenograft (PDX) Models

Xiaohui Zhou
Nanjing Medical University https://orcid.org/0000-0001-7436-7110
Yeqing Gong
Nanjing Medical University
Xiaorong Liu
Nanjing Medical University
Jiaqi Mao
Nanjing Medical University
Zhen Chen
Nanjing Medical University
Tingting Zhou
Nanjing Medical University
Chao Chen
Nanjing Medical University
Yunfen Hua
Zhejiang University of Technology
Xin Shi
Southeast University Zhongda Hospital Department of General Surgery
Liu Yang
Jiangsu Institute of Cancer Research: Jiangsu Cancer Hospital
Fan Lin (linfee@me.com)
Nanjing Medical University https://orcid.org/0000-0001-9169-9416

Research

Keywords: Palbociclib, Erlotinib, Colorectal cancer, CDK4/6, KRAS

Posted Date: January 7th, 2021

DOI: https://doi.org/10.21203/rs.3.rs-139687/v1

Abstract

Background: The heterogenetic nature of colorectal cancer (CRC) constitutes a major challenge for drug development. Simultaneous targeting multiple molecules by combination therapy provides a promising strategy, but it requires identification of more potentially useful targeted agents. Palbociclib, a selective CDK4/6 inhibitor approved for the treatment of HR/ER-positive and HER2-negative breast cancer, exhibited anti-cancer versatility in several types of cancer. In this study, we evaluated its usefulness in the treatment of CRC either by single-agent or combined with a small molecule EGFR inhibitor erlotinib.

Methods: The impacts of palbociclib, erlotinib, and their combination on cell proliferation, colony formation, cell cycle, apoptosis, senescence, and ROS accumulation in CRC cells were assessed. Their efficacies were evaluated in CRC patient-derived organoids (PDO) and xenograft (PDX) models.

Results: Single-agent palbociclib efficiently inhibited proliferation, suppressed the RB phosphorylation, and caused G1-phase arrest in KRAS/BRAF mutated CRC cell lines. IC50 of all cell lines were below 1 μM. Moreover, it induced ROS accumulation and consequently caused apoptosis and senescence of CRC cells. The addition of erlotinib further aggravated palbociclib-induced anti-proliferation, cell cycle arrest, ROS accumulation, apoptosis, and senescence via blocking multiple critical effectors on RB/PI3K/RAS pathways and such interaction between two agents are synergistic. Finally, both palbociclib and erlotinib demonstrated anti-CRC activities, but only their combination caused statistically meaningful inhibition of tumor growth and prolonged survival with tolerable toxicity in KRAS wildtype/mutated PDX models.

Conclusion: Our work demonstrated that the palbociclib and erlotinib combination treatment is a promising therapy for CRC and worthy of further clinical evaluation.

Background

Colorectal cancer (CRC) is a leading cause of cancer death in the world. About 1.84 million new cases of CRC are diagnosed annually, ranking the third and second in the incidence of malignant tumors in men and women [1]. Detection of CRC at an early stage may lead to a 90% five-year survival rate [2], whereas most of the diagnosed cases were found at an advanced stage. Palliative treatment is the main method for advanced metastatic CRC with limited overall therapeutic effect and a five-year survival rate of just 12% [3]. Therefore, development of novel and effective therapeutics for CRC is in dire need.

CRC is a highly heterogeneous type of cancers by nature. It means the increase of the complexity in genetic mutations, epigenetic regulation, and tumor microenvironment, and ultimately these constitute a critical challenge for the development of targeted therapeutics for CRC [4, 5]. Hence an ideal targeted therapy for CRC should be both potent and versatile. In recent years, a new generation of CDK (cyclin-dependent kinases) inhibitors with improved selectivity for CDK4 and CDK6 paves a new way for cell cycle targeted therapeutics and showed promised efficacy in several types of cancer [6]. CDK 4 and 6 bind with Cyclin D to form Cyclin D-CDK4/6 complexes which promote phosphorylation and inactivation of the tumor suppressor retinoblastoma protein (Rb), thus releasing E2F transcription factor to increase

transcription of genes promoting cell cycle progression from G1 into S phase [7]. A highly selective small molecular inhibitor of CDK4/6, palbociclib (PD0332991) has been approved by the FDA in 2015 for the first-line treatment of postmenopausal women with HR/ER-positive and HER2-negative advanced breast cancer in combination with letrozole as initial hormone-plus CDK-targeted therapy [8]. Although genetic aberrations in cyclin/CDK elements in CRC are rare [9], cyclin D1 [10, 11] is frequently overexpressed and causes cell cycle dysregulation. Interestingly, further studies revealed that palbociclib has CDK4/6 independent mechanisms to induce senescence[12], apoptosis [13], and sensitize radiotherapy [14] and targeted therapy [15]. Due to the limited studies, whether palbociclib is useful in treating CRC is yet unknown, so our first aim is to evaluate the usefulness of palbociclib in preclinical CRC models.

The epidermal growth factor receptor (EGFR), a well-established oncogenic driver, is overexpressed in 60–80% of CRC and provides an important target for drug intervention [16]. Nevertheless, the current anti-EGFR therapy composed of the EGFR antibodies (cetuximab or panizumab) in combination with fluorouracil (5-FU) plus irinotecan (FOLFIRI) and 5-FU plus oxaliplatin (FOLFOX) only benefits the patients with RAS wild-type metastatic CRC, and even in these patients not all of them respond to therapy because of alternative resistance mechanisms [17]. Erlotinib (Tarceva, OSI-774) is a potent small-molecule EGFR tyrosine kinase inhibitor approved in the treatment of advanced pancreatic cancer and non-small cell lung cancer. It was previously evaluated in CRC treatment and showed tolerated toxicity [18] and marked reduction in phosphorylated EGFR and EGFR-mediated functions [19]. In esophageal squamous cell carcinoma, erlotinib combined with palbociclib exhibited a cheerful outcome *in vivo* [20]. Therefore, our second aim is to assess whether palbociclib and erlotinib have synergistic interaction and enhance the anti-tumor activity by each other in CRC models. Our data supported the usefulness of palbociclib in the treatment of CRC and demonstrated the significant effects of combined treatment of palbociclib and erlotinib even in both KRAS wild-type and mutated CRC models.

Materials And Methods

Cell lines and drug treatment. Human CRC cell lines (HT29, HCT116, HCT15, DLD1, LOVO) were obtained from the Cell Bank of the Chinese Academy of Sciences (Shanghai, China). All the above cell lines were authenticated by Biowing Biotech (Shanghai, China). HT29, HCT116, and LOVO were cultured in DMEM (Gibco, CA, USA) supplemented with 10% fetal bovine serum (FBS, VACCA, Shanghai, China) and 100 μg/mL penicillin/streptomycin (Invitrogen). The rest of the cell lines were grown in RPMI-1640 medium (Gibco) with the same supplements. All cells were cultured in a humidified incubator with 5% of carbon dioxide (CO_2) and 95% air at 37 °C and were routinely checked for mycoplasma by PCR. Palbociclib and erlotinib were purchased from MedChemExpress Chemicals. Drugs were dissolved in DMSO at 200 μM and 10 mM stock solution concentration and stored in aliquots at − 80 °C.

Animals. Mice were housed and handled according to institutional guidelines complying with local legislation. All experiments with animals were approved by the animal experiment committee of the Nanjing Medical University. NOD/ShiLtJGpt-*Prkdc*^{em26Cd52}*Il2rg*^{em26Cd22}/Gpt (NCG, female, 3–4 weeks,

18–20 g) mice were purchased from Jiangsu GemPharmtech co., ltd (Nanjing, China) and were adapted to the environment for a week before the experiment.

Anti-proliferation and clonogenic assays. The cells were seeded in 96-well plates at a density of 2000 cells per well one night before 72 h drug treatment. Proliferation rates of CRC cells were determined using an Alamar Blue assay (Yeasen, Shanghai, China). Drug interaction analysis was performed using the Chou-Talalay method [21]. The combination index (CI) was calculated by the CompuSyn program (ComboSyn Inc). For the clonogenic assay, cells were seeded in 12-well plates at a density of 400–1000 cells per well. Drug containing medium was refreshed every 3–4 days. Cells were fixed after 10–14 days of treatment and stained with a Giemsa staining solution (KeyGEN Biotech, Nanjing, China). The number and density of colonies were quantified using Image J.

Flow Cytometry Analysis of Cell Cycle, Apoptosis, and ROS level of CRC cells. Cells were seeded at 1×10^5 cells per well in 6-well plates and were incubated overnight. For cell cycle analysis, the cells were synchronized by starving in serum-free DMEM for 24 h before treatment. Then the cells were treated with palbociclib, erlotinib, or their combination for 72 h and were collected by trypsinization into ice-cold PBS followed with brief centrifugation. For cell cycle analysis, the above-collected cell pellets were fixed in 75% ethanol for 2 h and resuspended in 1% (w/v) bovine serum albumin in PBS. Next, the cells were stained with propidium iodide (PI) at a final concentration of 0.1 mg/ml together with 0.1 mg/mL RNaseA (20 g/mL) at 37 °C for 15 min in the dark. For apoptosis analysis, 1×10^5 drug-treated cells were stained with Annexin V-APC and propidium iodide (PI) using an Apoptosis Detection Kit (Yeasen Biotech, Shanghai) at room temperature for 15 min. For ROS measurement, the cells were incubated with 10 μM DCFH-DA (Solarbio Life Science, Beijing, China) at 37 °C for 30 min in the dark and then washed with PBS. The stained cells from the above treatments were subjected to flow cytometric analysis using a FACS Calibur (BD Biosciences) flow cytometer, and data were analyzed by FlowJo 7.6.

Western blotting. Cells were lysed in RIPA buffer supplemented with protease inhibitors (50 mmol/L Tris-HCl, pH 8.0, 150 mmol/L sodium chloride, 1.0% NP-40, 0.5% sodium deoxycholate, and 0.1% SDS). The equal amount of proteins (15–20 μg) were loaded on SDS-PAGE gels and separated by electrophoresis. After transferring the protein to a PVDF membrane (Merck Millipore, MA, USA), it was blocked with 3% BSA and incubated with appropriate primary and secondary antibodies. The following primary antibodies were used in the study: pEGFR (Tyr1068) (#3777T), pAKT (Ser473) (#4060), AKT (#9272), pERK1/2 (Thr202/204) (#4370), pMEK1/2 (#2338), pRB (Ser807/811) (#8516), RB (#9309), GSK3β (#12456), pGSK3β (Ser9) (#9323) and FoxM1 (#5436) (Cell Signaling Technology); p4EBP1 (Ser65) (#SC293124, Santa Cruz Biotechnology, CA, USA), GAPDH (#AC002) (ABclonal, Hubei, China). At last, the blots were detected after exposure to the enhanced chemiluminescence kit using a ChemiDoc MP imaging system.

Patient-derived CRC organoids and xenografts. CRC specimens were acquired from patients in routine operation after obtaining fully informed consent according to Jiangsu Cancer Hospital. The CRC organoids were established according to the protocol developed by Hans Clevers lab [22]. In brief, fresh surgically resected CRC tissues were minced into 1 mm^3 fragment and digested with 1 mg/mL

collagenase A (Sigma, #C0130, USA) at 37 °C for 30 min. After brief centrifugation, the pellet was resuspended in PBS and was mechanically dissociated by repetitive pipetting. The isolated cells/fragments were passed through a 70 μm cell strainer, centrifuged, and resuspended in matrigel (Corning, #354230, USA) at 1×10^6 cells per mL. The mixture was dispensed as 25 μl per drop and seeded into each well in 24-well plates and was solidified in a 37 °C incubator for 10 min. 500 μl of culture medium composed of DMEM/F-12 (Hyclone) supplemented with 1 × penicillin/streptomycin, 10 mM HEPES (Invitrogen), 2 mM GlutaMAX (Invitrogen), 1 × B27 (Invitrogen), 1 × N2 (Gibco), 1 mM N-Acetylcysteine (Sigma) together with niche factors: 50 ng/mL for EGF (Thermo Fisher Scientific/Gibco #PHG0313), 500 nM for TGF-β receptor type I inhibitor A83-01 (MCE, #HY-10432) and 10 μM for p38 MAP kinase inhibitor SB202190 (MCE, # HY-10295) was added into each well. 10 mM Y-27632 dihydrochloride kinase inhibitor (MCE, # HY-10071) was also added for the first 2 days. After the successful formation of CRC organoids, palbociclib, erlotinib, or their combination was added into the culture medium to evaluate their effects.

For the PDX model, 4–5 weeks female immunodeficient NCG mice [23] were used as the recipient of patient-derived CRC tissue. Fresh surgically resected CRC tissues from two CRC patients (P328 and P44) were minced into approximately 3 mm^3 fragments and subcutaneously engrafted into the right region of each mouse. When tumors reached a volume of 80–120 mm^3, the mice were separated randomly into 4 groups. The P328 PDX cohort including 20 tumor-bearing mice (five in each group) received erlotinib (resuspended in 6% Captisol; 50 mg/kg), palbociclib [resuspended in sodium(S)-lactate buffer (50 mmol/L, pH 4.0); 25 mg/kg], or their combination and the P44 PDX cohort including 37 tumor-bearing mice (8–10 in each group) received erlotinib (25 mg/kg), palbociclib (25 mg/kg), or their combination, respectively, by oral gavage 5 days a week for more than 4 weeks. The mice were weighed every 2 days and monitored for tumor volume (Length × $Width^2$ × 0.5) until the tumor reached the maximum authorized ethical volume of 2500 mm^3 or if their health severely deteriorated (censored event).

β-Gal staining. The intracellular β-galactosidase level was determined using a Cell Senescence Testing Kit (GenMed Scientifics Inc. MN, USA). The staining procedure was followed by the manufacture's instructions. Briefly, CRC cells pre-seeded in 12-well plates were treated with palbociclib, erlotinib, or their combination for 72 h and incubated with the Fixative Solution, washed, and incubated with Staining Solution for 16 h at 37 °C. Then the cells were washed with PBS three times and observed with a Zeiss microscope. β-galactosidase positive cells were counted and the numbers from eight representative fields of three independent experiments were calculated.

Statistical analysis. The *in vitro* data in figures are represented as the mean ± SD and the data of PDX tumor growth are presented as mean ± SEM (standard error of the mean). Statistical significance was calculated by Student's t-test or ANOVA using GraphPad Prism. *In vitro* experiments were performed in triplicate and replicated in more than two independent experiments. The statistical significance of differences is indicated in figures by asterisks as follows: *, $p < 0.05$; **, $p < 0.01$; and ***, $p < 0.001$.

Results

Palbociclib exhibited antitumor activity and targeted inhibition in CRC cells.

We started with anti-proliferation and clonogenic assays to evaluate the effectiveness of palbociclib in multiple CRC cell lines. Despite the differences across five KRAS/BRAF mutated CRC cell lines, palbociclib exhibited dose-dependent anti-proliferative and colony formation inhibitory effects. The half inhibitory doses of all CRC cell lines were below 1 μM, suggesting its excellent potency and potential usefulness for CRC cells including those carrying KRAS/BRAF mutation (Fig. 1a and b). Figure 1c listed the mutations of the RAS and RAS related pathway of the above CRC cell lines. As a CDK4/6 inhibitor, treatment of palbociclib successfully reduced the levels of phosphorylated RB and FoxM1, another downstream target phosphorylated and stabilized by CDK4/6, [24], and also caused a dose-dependent reduction of RB protein (Fig. 1d).

Palbociclib induced dose-dependent cell cycle arrest, apoptosis, senescence-like phenotype, and ROS accumulation in CRC cells.

To investigate the mechanism of growth inhibitory effect of palbociclib in both short-term (anti-proliferation assay) and long-term (clonogenic assay) treatment, we analyzed the impact of palbociclib on CRC cell cycle, apoptosis, and senescence. Consistent with a CDK4/6-targeted mechanism, palbociclib successfully caused significant G1-pahse arrest even at a low concentration of 0.1 μM and aggravated the cell cycle blockage with dose increasing in HT29 and HCT116 cells (Fig. 2a and b). Moreover, in line with Thoms and coworkers' findings, a low dose of palbociclib also induced significant apoptosis in the CRC cell lines, suggesting alternative CDK4/6 downstream pathways than the classic cyclin D-CDK4/6-Rb pathway are involved (Fig. 2c and d) [13]. We wondered whether palbociclib also causes irreversible senescence in CRC cells as previous work indicated [24]. Indeed, palbociclib treated CRC cells demonstrated typical senescence phenotypes, including enlarged cytoplasm, abnormal nucleus, and dose-depending increase of β-Galactosidase staining (Fig. 2e and f). Lastly, we found that the ROS level was raised markedly after a short (1 day) or long (7 days) treatment duration of palbociclib, suggesting that ROS accumulation could be responsible for palbociclib-induced apoptosis and senescence (Fig. 2g and h).

The combination of palbociclib and erlotinib (PE-combination) synergistically inhibited the growth of CRC cells and organoids.

Erlotinib, an FDA-approved EGFR inhibitor for treatment of lung and pancreatic cancer, showed tolerable toxicity and blockage of EGFR and EGFR mediated functions in previous CRC trials. As shown in Fig. 3a and b, the addition of erlotinib significantly enhanced the anti-proliferation activity of palbociclib in different CRC cell lines. Isobologram and CI value analysis revealed that the interaction between the PE-combination was synergistic (CI value < 1 indicated a synergistic interaction, Fig. 3c). Moreover, HSA synergy matrices generated by Combenefit [25] showing that most of the synergy scores of PE-

combinations were above 0, indicating a general synergistic interaction between the PE-combination in CRC cells (Fig. 3d).

Next, we used the clonogenic assay to evaluate the long-term effect of PE-combination. In result, PE-combination significantly reduced colony formation of CRC cells compared with single-drug treatment even at relatively low concentrations (Fig. 3e and f). Patient-derived organoids (PDO) have been approved to be a more reliable model to predict the drug response than established cell lines as it recapitulates the genomic and microenvironmental characteristics of CRC [26]. We took advantage of the tumor tissue derived from a CRC patient with poorly differentiated adenocarcinoma and cultured it in the organoid medium. The formation of normal organoids was severely impaired after treatment of 1 μM palbociclib or 10 μM erlotinib and was further aggravated upon the treatment of both drugs (Fig. 3g).

The addition of erlotinib to palbociclib treatment aggravated cell cycle arrest, apoptosis, and suppression of multiple oncogenic pathways.

To explore the synergistic mechanism between palbociclib and erlotinib, we investigated the impacts of PE-combination on cell cycle, apoptosis, and relevant signaling pathways. Again, single-agent palbociclib caused strong cell cycle arrest at the G1 phase. Although erlotinib alone had a marginal effect on cell cycle, the addition of erlotinib to palbociclib further aggravated the G1-phase arrest (Fig. 4a and b). Moreover, the addition of erlotinib also significantly enhanced palbociclib-induced apoptosis in CRC cells (Fig. 4c and d). Importantly, the immunoblotting analysis revealed that PE-combination potently inhibited several critical pathways even at relatively low concentration (palbociclib: 20 nM; erlotinib: 2 μM): Firstly, the levels of total RB, p-RB, and FoxM1 were significantly suppressed by PE-combination relative to single-agent treated cells; Secondly, EGFR and its downstream components in PI3K and RAS pathways including p-ERK, p-AKT, p-GSK3β and p-4EBP1 were all effectively suppressed by PE-combination. Despite the variation across three cell lines, PE-combination successfully attenuated signaling in RB, PI3K and RAS pathways which are determinants of cell proliferation and growth (Fig. 4e).

Erlotinib enhanced palbociclib-induced senescence and ROS accumulation.

Next, we investigated whether the addition of erlotinib to palbociclib causes a synergetic induction of a senescence-associated β-galactosidase phenotype in CRC cells. As shown in Fig. 5a-d, quantitative analysis of β-galactosidase positive cells revealed that erlotinib alone had a very limited effect to induce a senescence phenotype, whereas PE-combination significantly elevated the proportion of β-galactosidase positive cells relative to those treated by palbociclib alone in HT29 (Fig. 5a and b) and HCT116 cells (Fig. 5c and d). We also measured the ROS levels in CRC cells treated by palbociclib, erlotinib, or PE-combination. Both direct visualization (Fig. 5e) and FACS quantification of DCFH-DA (a florescent oxidant-sensing probe) stained cells (Fig. 5f and g) showed that PE-combination significantly enhanced ROS accumulation compared with single drug in the treatment of CRC cells. Such a high level of ROS at least partially explains the additional elevation of apoptosis and senescence caused by treatment of PE-combination.

PE-combination exhibited significant in vivo **efficacy in PDX models**

To evaluate the efficacy of palbociclib and PE-combination *in vivo*, we took advantage of the two PDX models established in our lab. P328 PDX was derived from a 54-year-old female CRC patient diagnosed with stage IV poorly differentiated mucinous colorectal adenocarcinoma and it has a wild-type KRAS gene. P44 PDX was derived from a 28-year-old female CRC patient diagnosed with poorly differentiated tubular/papillary adenocarcinoma with vessel, posterior wall of rectum, and liver metastases and its KRAS gene contains a G13D mutation (Fig. 6a). For P328 PDX, treatment of palbociclib (25 mg/kg) combined with erlotinib (50 mg/kg) led to a 2.9-fold reduction of tumor volume at day 26 when the endpoint of the experiment was reached (Fig. 6b and d). Single-agent treatment of palbociclib and erlotinib caused a 1.6-fold and a 1.4-fold reduction of tumor volume, respectively, but the differences compared with the control group were not statistically significant. Meanwhile, mice that received the PE-combination experienced 9–26% body weight losses (Fig. 6c).

Next, we reduced the dose of erlotinib to 25 mg/kg and tested the drug effect in the KRAS-mutated P44 PDX model. Again, mice that received PE-combination showed significant tumor growth suppression (2.7-fold reduction, $p = 0.011$, Fig. 6e and h) and prolonged survival ($p < 0.0001$, Fig. 6g) compared with those in the control group. Although single-agent treatment by palbociclib or erlotinib again did not show statistically different results in tumor growth control, palbociclib but not erlotinib significantly improved the overall survival ($p = 0.0358$) relative to the control group. At this dosage regimen, most treated mice including those received PE-treatment recovered from an initial period of body weight loss and showed no prolonged toxicity ever since (Fig. 6f). Finally, H&E and Ki-67 staining showed that the tumor tissue isolated from PE-combination treated mice contained more necrotic region and less Ki-67 positive proliferative cells compared with those from the control group (Fig. 6i).

Discussion

In the present study, we first evaluated the potential usefulness of palbociclib in the treatment of CRC to know the single-agent effect of palbociclib and the mechanism to suppress the growth of CRC cells. In result, palbociclib did efficiently inhibited the proliferation and growth of CRC cells, but it was not only because of cell cycle arrest, also due to its activity to induce senescence and apoptosis. This could be advantageous for potential CRC therapy because both senescence and apoptosis are irreversible processes of cell fate. For stage II and III CRC patients, the five-year recurrence rate is high (9–22% for stage II and 17–44% for stage III, respectively) [27], so a desired targeted therapy should not only be able to control the tumor progression but also reduce the recurrence rate of CRC.

Combination therapy is commonly used in treating cancers to improve the therapeutic effect of single-agent therapy, reverse the drug resistance, and help to reduce the unnecessary high dose of individual drugs to avoid the potential toxicity caused by the off-target effect [28]. Despite the promising activities of palbociclib, previous clinical trials showed that de novo and acquired resistance developed during palbociclib treatment [29]. Regarding the highly heterogeneous nature of CRC, it is less likely that the

single-agent palbociclib can completely control the disease progression even though it exhibited a promising anti-tumor effect in our preclinical models. Recently, two groups tested the effects of palbociclib combined with MEK inhibitor Trametinib or PD0325901 to treat KRAS mutant CRC. Despite that the combined therapy of palbociclib and Trametinib/PD0325901 demonstrated remarkable anti-tumor effects, both groups mentioned that severe toxicity developed during the combination treatment [30, 31]. In comparison, EGFR inhibitor erlotinib is extensively used for the clinical treatment of EGFR mutated tumors and showed relatively tolerable and controllable side effects. Moreover, EGFR is a critical driver gene affecting multiple downstream oncogenic pathways, so targeting EGFR instead of MEK not only blocks the RAS signaling, but also effectively suppresses PI3K-AKT, SRC, PLC-γ1-PKC, JNK, and JAK-STAT pathways [32]. In fact, EGFR antibodies in combination with fluorouracil (5-FU) plus irinotecan (FOLFIRI) and 5-FU plus oxaliplatin (FOLFOX) have shown significantly improved survival in KRAS wild-type CRC. Importantly, when the NF1 is competent, KRAS G13D-Mutated CRC cells are still benefited from the treatment or erlotinib or other EGFR inhibitors [33], so EGFR instead of MEK should be an appropriate target for this subset of CRC.

Another strength of this study is that we used clinically relevant PDO and PDX models for the drug efficacy study. The traditional cell-derived xenografts models were frequently used in drug efficacy studies, but they rarely predicted clinical response adequately [34]. PDX model well recapitulates cellular heterogeneity and molecular characteristics of primary CRC cancer and provides a better tool to predict the drug response than cell-derived xenografts [35, 36]. Consistent with previous clinical studies [18], single-agent erlotinib exhibited modest anti-CRC activity but such an effect failed to cause a statistical difference in tumor volume or survival. In addition, treatment of single-agent palbociclib led to improved survival relative to control group, but the improvement was limited (Median survival 27 *vs.* 19 days). Nevertheless, the results from PE-combination treatment convincingly revealed the potent anti-tumor effect in P328 (KRAS wt) and P44 (KRAS G13D) and marked prolongation of survival in P44 (KRAS G13D) PDX models (Median survival 35 *vs.* 19 days).

Conclusions

Collectively, these data provide vigorous evidence that palbociclib is a potential targeted agent to treat CRC and its anti-tumor activity can be further enhanced by combining with erlotinib. By simultaneously blocking EGFR and CDK4/6-RB signaling, the two targeted agents demonstrated synergistic anti-tumor effects in KRAS mutated CRC models. Given the fact that both palbociclib and erlotinib are FDA-approved drugs, further evaluation of the PE-combination in the clinical setting should be feasible and interesting.

Abbreviations

CRC: Colorectal cancer

ROS: Reactive oxygen species

DMSO: Dimethylsulfoxide

PDX: Patient-derived xenograft

PDO: Patient-derived organoids

CI: Combination index

EGFR: Epidermal growth factor receptor

CDK: Cyclin-dependent kinases

DCFH-DA: 2',7'-Dichlorodihydrofluorescein diacetate

Declarations

Availability of data and materials

The analysed data sets generated during the study are available from the corresponding author on reasonable request.

Funding

This study was supported by the National Natural Science Foundation of China (81672962), the Jiangsu Provincial Innovation Team Program Foundation, and the Joint Key Project Foundation of Southeast University and Nanjing Medical University.

Ethics declarations

All experiments with animals were approved by the animal experiment committee of the Nanjing Medical University. CRC specimens were acquired from patients in routine operation after obtaining fully informed consent according to Jiangsu Cancer Hospital. Besides, the patient's privacy has been fully protected.

Consent for publication

The content of this manuscript has not been previously published and is not under consideration for publication elsewhere and it has been read and approved by all the co-authors.

Conflict of interest

The authors disclose no potential conflicts of interest.

Authors' Contributions: Conceptualization: Fan Lin, Liu Yang, Xin Shi; Methodology: Fan Lin, Yunfeng Hua; Formal analysis and investigation: Xiaohui Zhou, Yeqing Gong, Xiaorong Liu, Jiaqi Mao, Zhen Chen, Chao Chen; Writing - original draft preparation: Xiaohui Zhou, Yeqing Gong; Writing - review and editing: Fan Lin; Funding acquisition: Fan Lin, Liu Yang; Resources: Liu Yang; Supervision: Fan Lin, Tingting Zhou

References

1. Bray F, Ferlay J, Soerjomataram I, et al. Global cancer statistics 2018: GLOBOCAN estimates of incidence and mortality worldwide for 36 cancers in 185 countries. CA Cancer J Clin. 2018; 68:6394-424.
2. Siegel RL and Miller KD. Cancer statistics, 2019. 2019; 69:17-34.
3. Wolf AMD, Fontham ETH, Church TR, et al. Colorectal cancer screening for average-risk adults: 2018 guideline update from the American Cancer Society. CA Cancer J Clin. 2018; 68:4250-281.
4. Molinari C, Marisi G, Passardi A, et al. Heterogeneity in Colorectal Cancer: A Challenge for Personalized Medicine? Int J Mol Sci. 2018; 19:12.
5. Sagaert X, Vanstapel A and Verbeek S. Tumor Heterogeneity in Colorectal Cancer: What Do We Know So Far? Pathobiology. 2018; 85:1-272-84.
6. Goel S, DeCristo MJ, McAllister SS and Zhao JJ. CDK4/6 Inhibition in Cancer: Beyond Cell Cycle Arrest. Trends Cell Biol. 2018; 28:11911-925.
7. Kato J, Matsushime H, Hiebert SW, Ewen ME and Sherr CJ. Direct binding of cyclin D to the retinoblastoma gene product (pRb) and pRb phosphorylation by the cyclin D-dependent kinase CDK4. Genes Dev. 1993; 7:3331-42.
8. Beaver JA, Amiri-Kordestani L, Charlab R, et al. FDA Approval: Palbociclib for the Treatment of Postmenopausal Patients with Estrogen Receptor-Positive, HER2-Negative Metastatic Breast Cancer. Clin Cancer Res. 2015; 21:214760-6.
9. Kato S, Schwaederle M, Daniels GA, et al. Cyclin-dependent kinase pathway aberrations in diverse malignancies: clinical and molecular characteristics. Cell Cycle. 2015; 14:81252-9.
10. Arber N, Hibshoosh H, Moss SF, et al. Increased expression of cyclin D1 is an early event in multistage colorectal carcinogenesis. Gastroenterology. 1996; 110:3669-74.
11. Bartkova J, Lukas J, Strauss M and Bartek J. The PRAD-1/cyclin D1 oncogene product accumulates aberrantly in a subset of colorectal carcinomas. Int J Cancer. 1994; 58:4568-73.
12. Miettinen TP, Peltier J, Hartlova A, et al. Thermal proteome profiling of breast cancer cells reveals proteasomal activation by CDK4/6 inhibitor palbociclib. EMBO J. 2018; 37:10.
13. Thoms HC, Dunlop MG and Stark LA. CDK4 inhibitors and apoptosis: a novel mechanism requiring nucleolar targeting of RelA. Cell Cycle. 2007; 6:111293-7.
14. Huang CY, Hsieh FS, Wang CY, et al. Palbociclib enhances radiosensitivity of hepatocellular carcinoma and cholangiocarcinoma via inhibiting ataxia telangiectasia-mutated kinase-mediated DNA damage response. Eur J Cancer. 2018; 10210-22.
15. Goel S, Wang Q, Watt AC, et al. Overcoming Therapeutic Resistance in HER2-Positive Breast Cancers with CDK4/6 Inhibitors. Cancer Cell. 2016; 29:3255-269.
16. Pabla B, Bissonnette M and Konda VJ. Colon cancer and the epidermal growth factor receptor: Current treatment paradigms, the importance of diet, and the role of chemoprevention. World J Clin Oncol. 2015; 6:5133-41.

17. Van Cutsem E, Cervantes A, Adam R, et al. ESMO consensus guidelines for the management of patients with metastatic colorectal cancer. Ann Oncol. 2016; 27:81386-422.
18. Townsley CA, Major P, Siu LL, et al. Phase II study of erlotinib (OSI-774) in patients with metastatic colorectal cancer. Br J Cancer. 2006; 94:81136-43.
19. Mesange P, Bouygues A, Ferrand N, et al. Combinations of Bevacizumab and Erlotinib Show Activity in Colorectal Cancer Independent of RAS Status. Clin Cancer Res. 2018; 24:112548-2558.
20. Zhou J, Wu Z, Wong G, et al. CDK4/6 or MAPK blockade enhances efficacy of EGFR inhibition in oesophageal squamous cell carcinoma. Nat Commun. 2017; 813897.
21. Chou TC. Drug combination studies and their synergy quantification using the Chou-Talalay method. Cancer Res. 2010; 70:2440-6.
22. Koo BK, Stange DE, Sato T, et al. Controlled gene expression in primary Lgr5 organoid cultures. Nat Methods. 2011; 9:181-3.
23. Zhuang YP, Zhu YP, Wang HY, et al. Establishment of patient-derived tumor xenograft (PDTX) models using samples from CT-guided percutaneous biopsy. Braz J Med Biol Res. 2017; 50:6e6000.
24. Anders L, Ke N, Hydbring P, et al. A systematic screen for CDK4/6 substrates links FOXM1 phosphorylation to senescence suppression in cancer cells. Cancer Cell. 2011; 20:5620-34.
25. Di Veroli GY, Fornari C, Wang D, et al. Combenefit: an interactive platform for the analysis and visualization of drug combinations. Bioinformatics. 2016; 32:182866-8.
26. van de Wetering M, Francies HE, Francis JM, et al. Prospective derivation of a living organoid biobank of colorectal cancer patients. Cell. 2015; 161:4933-45.
27. Osterman E and Glimelius B Recurrence Risk. After Up-to-Date Colon Cancer Staging, Surgery, and Pathology: Analysis of the Entire Swedish Population. Dis Colon Rectum. 2018; 61:91016-1025.
28. Lehar J, Krueger AS, Avery W, et al. Synergistic drug combinations tend to improve therapeutically relevant selectivity. Nat Biotechnol. 2009; 27:7659-66.
29. Guarducci C, Bonechi M, Boccalini G, et al. Mechanisms of Resistance to CDK4/6 Inhibitors in Breast Cancer and Potential Biomarkers of Response. Breast Care (Basel). 2017; 12:5304-308.
30. Lee MS, Helms TL, Feng N, et al. Efficacy of the combination of MEK and CDK4/6 inhibitors in vitro and in vivo in KRAS mutant colorectal cancer models. Oncotarget. 2016; 7:2639595-39608.
31. Pek M, Yatim S, Chen Y, et al. Oncogenic KRAS-associated gene signature defines co-targeting of CDK4/6 and MEK as a viable therapeutic strategy in colorectal cancer. Oncogene. 2017; 36:354975-4986.
32. Wee P and Wang Z. Epidermal Growth Factor Receptor Cell Proliferation Signaling Pathways. Cancers (Basel). 2017; 9:5.
33. Rabara D, Tran TH, Dharmaiah S, et al. KRAS G13D sensitivity to neurofibromin-mediated GTP hydrolysis. Proc Natl Acad Sci U S A. 2019; 116:4422122-22131.
34. Voskoglou-Nomikos T, Pater JL and Seymour L. Clinical predictive value of the in vitro cell line, human xenograft, and mouse allograft preclinical cancer models. Clin Cancer Res. 2003; 9:114227-

39.

35. Bertotti A, Migliardi G, Galimi F, et al. A molecularly annotated platform of patient-derived xenografts ("xenopatients") identifies HER2 as an effective therapeutic target in cetuximab-resistant colorectal cancer. Cancer Discov. 2011; 1:6508-23.
36. Seol HS, Kang HJ, Lee SI, et al. Development and characterization of a colon PDX model that reproduces drug responsiveness and the mutation profiles of its original tumor. Cancer Lett. 2014; 345:156-64.

Figures

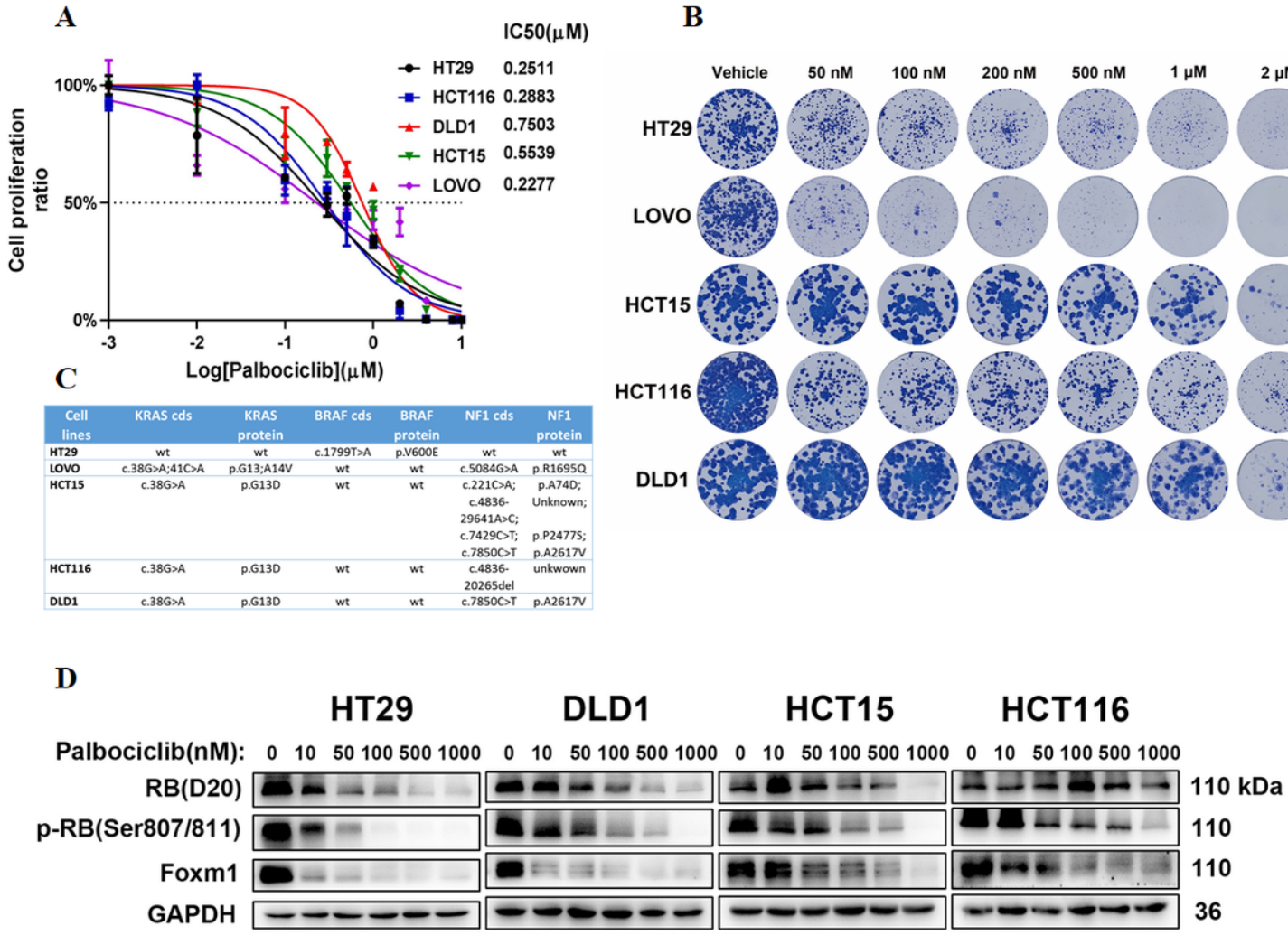

Figure 1

Evaluation of the anti-tumor effect and target inhibition of single-agent palbociclib in five CRC cell lines. (a) Palbociclib-induced inhibition of CRC cell proliferation. (b) Representative images of the colony-forming capacity of CRC cells upon treatment of palbociclib. (c) List of significantly mutated genes in RAS and related pathways of five CRC cell lines. (d) Immunoblotting analysis of the alterations of RB signaling pathway upon treatment of palbociclib.

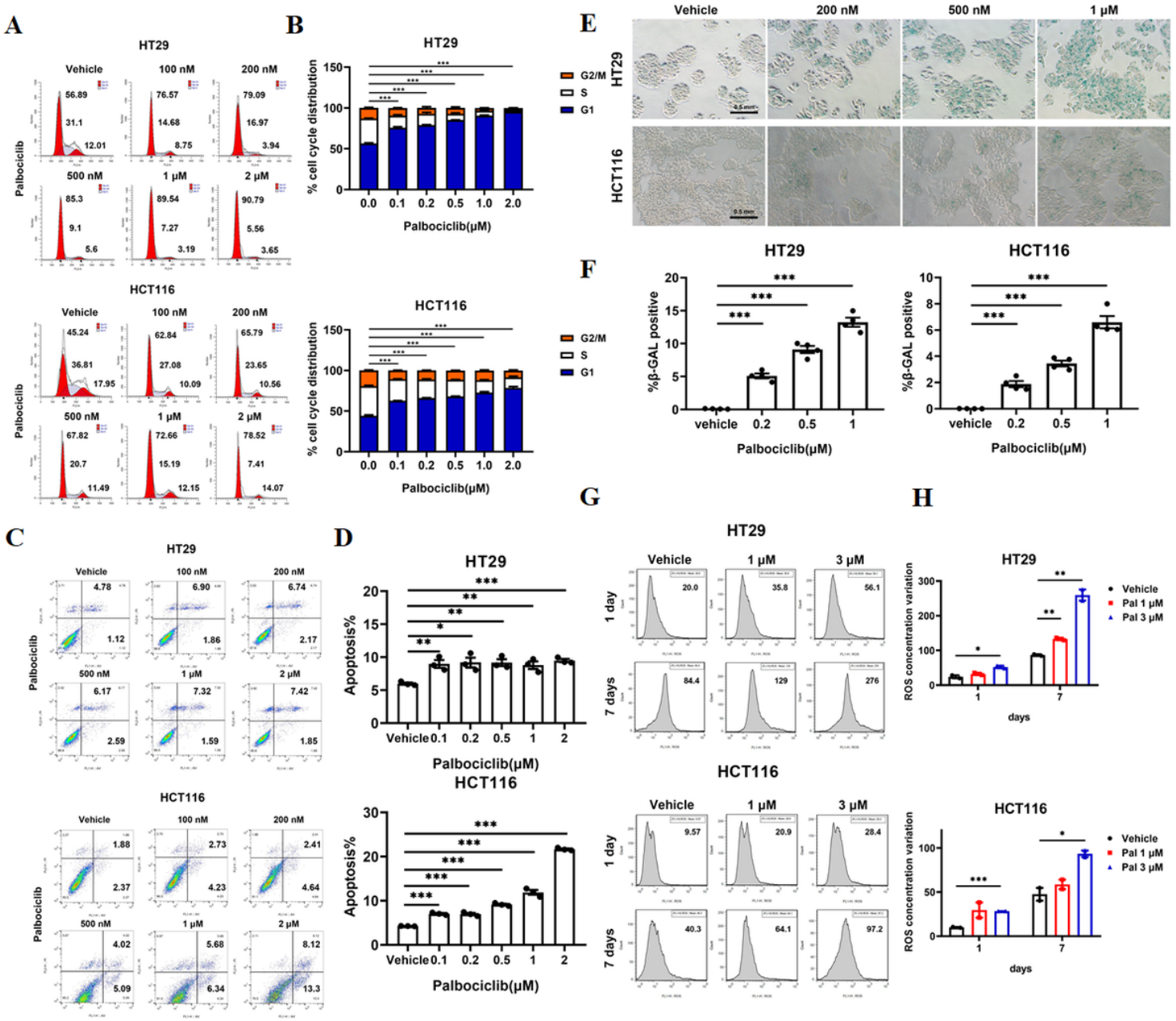

Figure 2

Palbociclib induced cell cycle arrest, apoptosis, senescence, and ROS accumulation in CRC cells. (a) Cell cycle analysis upon treatment of different concentrations of palbociclib. (b) The quantification of cell fractions in Sub-G1, S, and G2/M phases in (a). (c) Induction of apoptosis in cells treated with palbociclib. (d) Quantitation of (early and late) apoptotic cells induced by palbociclib in (c). (e) β-galactosidase staining in CRC cells treated with palbociclib. Scale bar, 0.5 mm. (f) Quantitation of the percentage of β-galactosidase-positive cells (by image J). (g) Flow cytometry analysis of CRC cells labeled with the ROS-sensitive dye DCFH-DA upon treatment of palbociclib. (h) Quantitation of the intracellular ROS levels in (g).

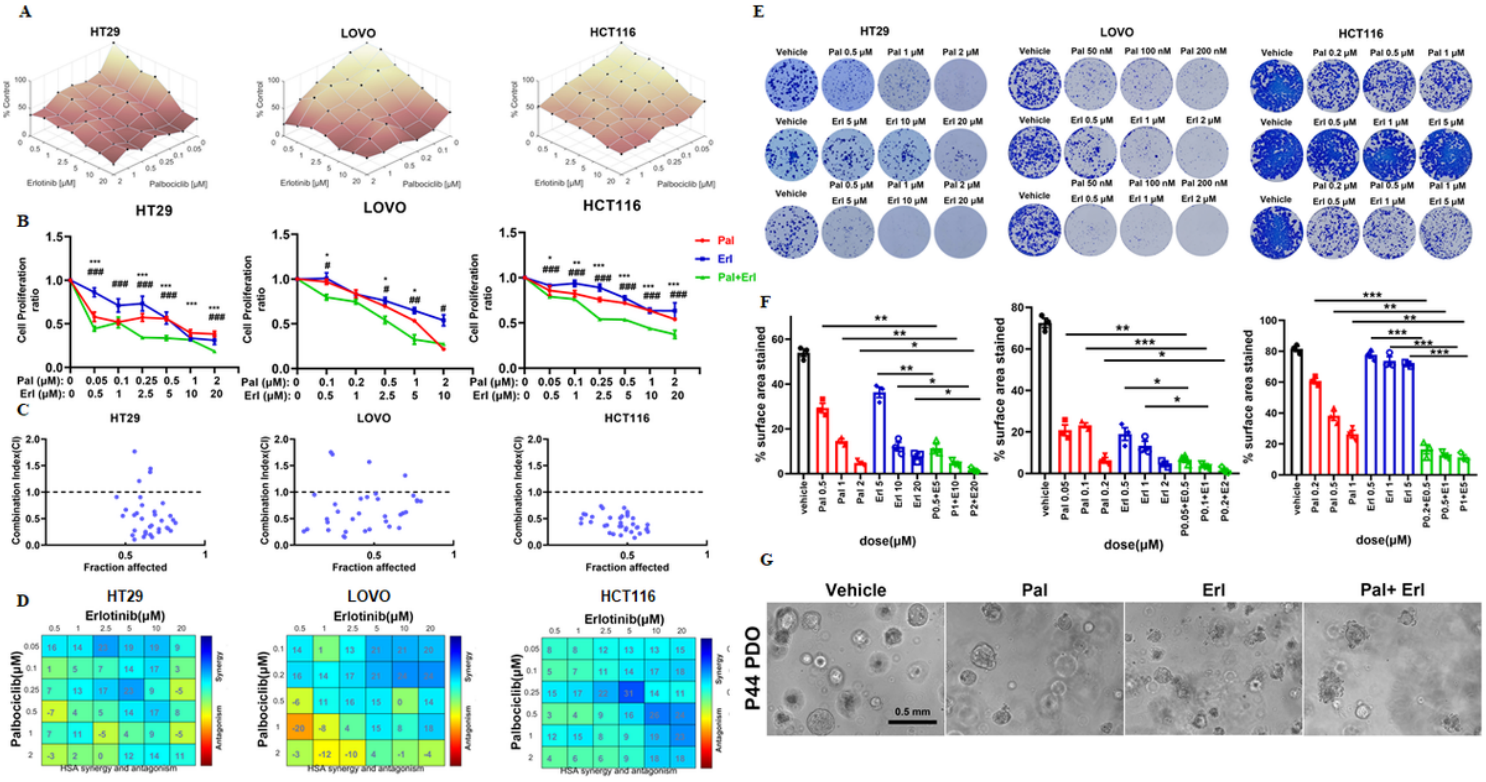

Figure 3

Determining the combined effects of palbociclib and erlotinib in proliferation, colony formation, and PDO formation. (a) Surface plots generated by dose-matrices of the proliferation rates up treatment of palbociclib and erlotinib at different concentrations. (b) The proliferation rate of three CRC cell lines treated with fixed concentration-combinations of palbociclib and erlotinib. (c) Analysis of the palbociclib and erlotinib interaction. the resulting fraction affected CI. CI plots showing the sturdy synergistic effect of palbociclib and erlotinib. CI < 1 indicates a synergistic effect. (d) HSA synergy matrices showing the interaction between palbociclib and erlotinib. HSA synergy score indicates the synergistic effects as calculated from expected and observed growth inhibition (> 0 indicate synergistic effects). (e) Colony formation of CRC cells treated with palbociclib and/or erlotinib. (f) Quantification of Giemsa staining positive cells in (e) by image J. (g) Representative images of PDOs (derived from P44) treated with palbociclib (1 μM) alone or in combination with erlotinib (10 μM). Scale bar, 0.5 mm.

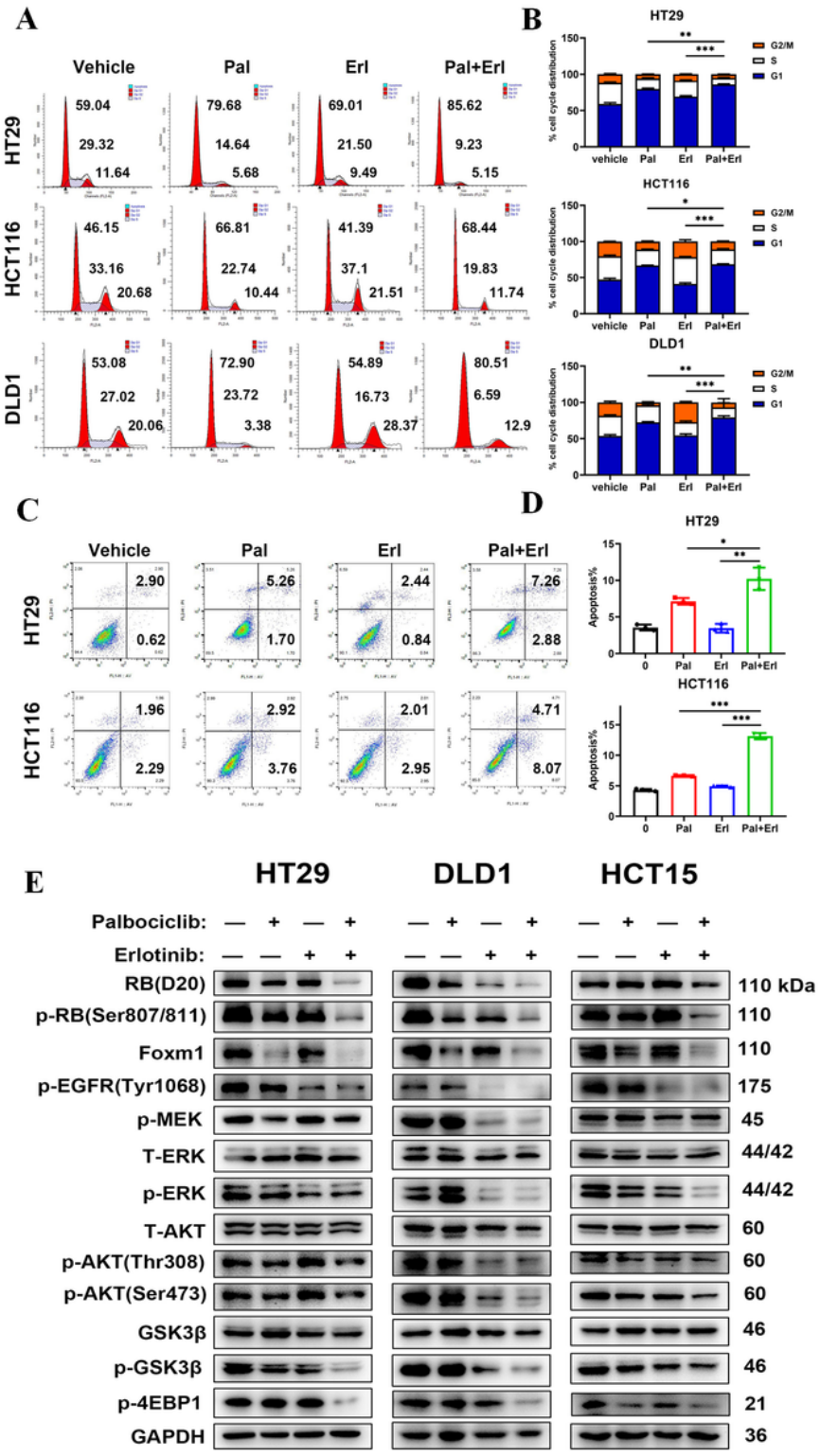

Figure 4

Erlotinib enhanced palbociclib-induced senescence, ROS accumulation, and inhibition of multiple oncogenic pathways. (a) Cell cycle and (c) apoptosis analysis upon treatment of palbociclib and erlotinib at different concentrations. (b) Quantitation of cells in different cell cycle phases in (a). (d) Quantitation of (early and late) apoptotic cells in (c). Immunoblotting analysis of the alterations of RB, RAS, and PI3K signaling pathways upon treatment of palbociclib and/or erlotinib.

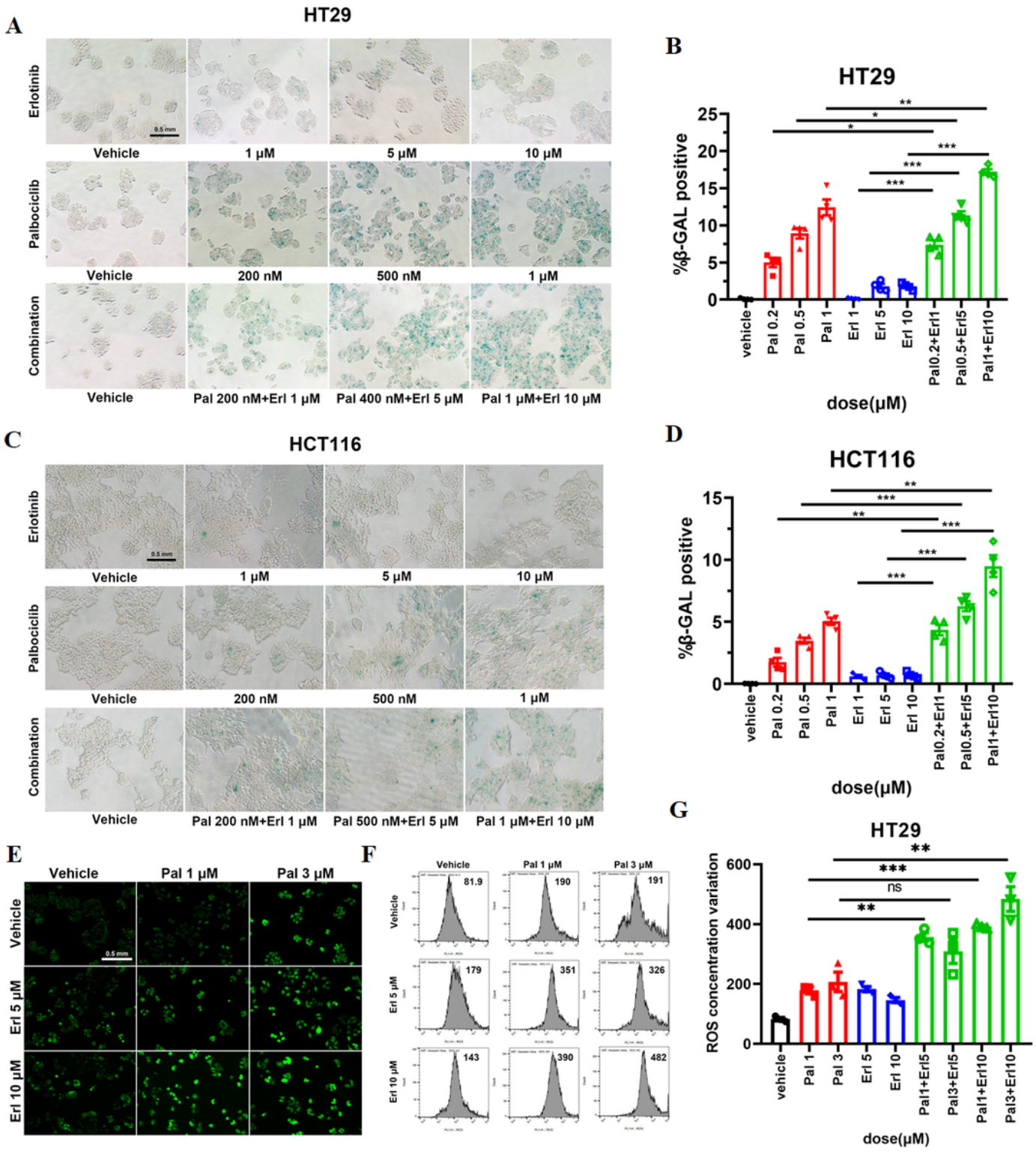

Figure 5

Induction of senescence and ROS in CRC cells treated with palbociclib and/or erlotinib. β-galactosidase staining in HT29 (a) and HCT116 (c) cells treated with palbociclib and/or erlotinib and their quantitation (b and d). Representative images captured by fluorescence microscope (e) or flow cytometry analysis (f) and its quantitation (g) of CRC cells labeled with the ROS-sensitive dye DCFH-DA upon treatment of palbociclib and/or erlotinib. Scale bar, 0.5 mm.

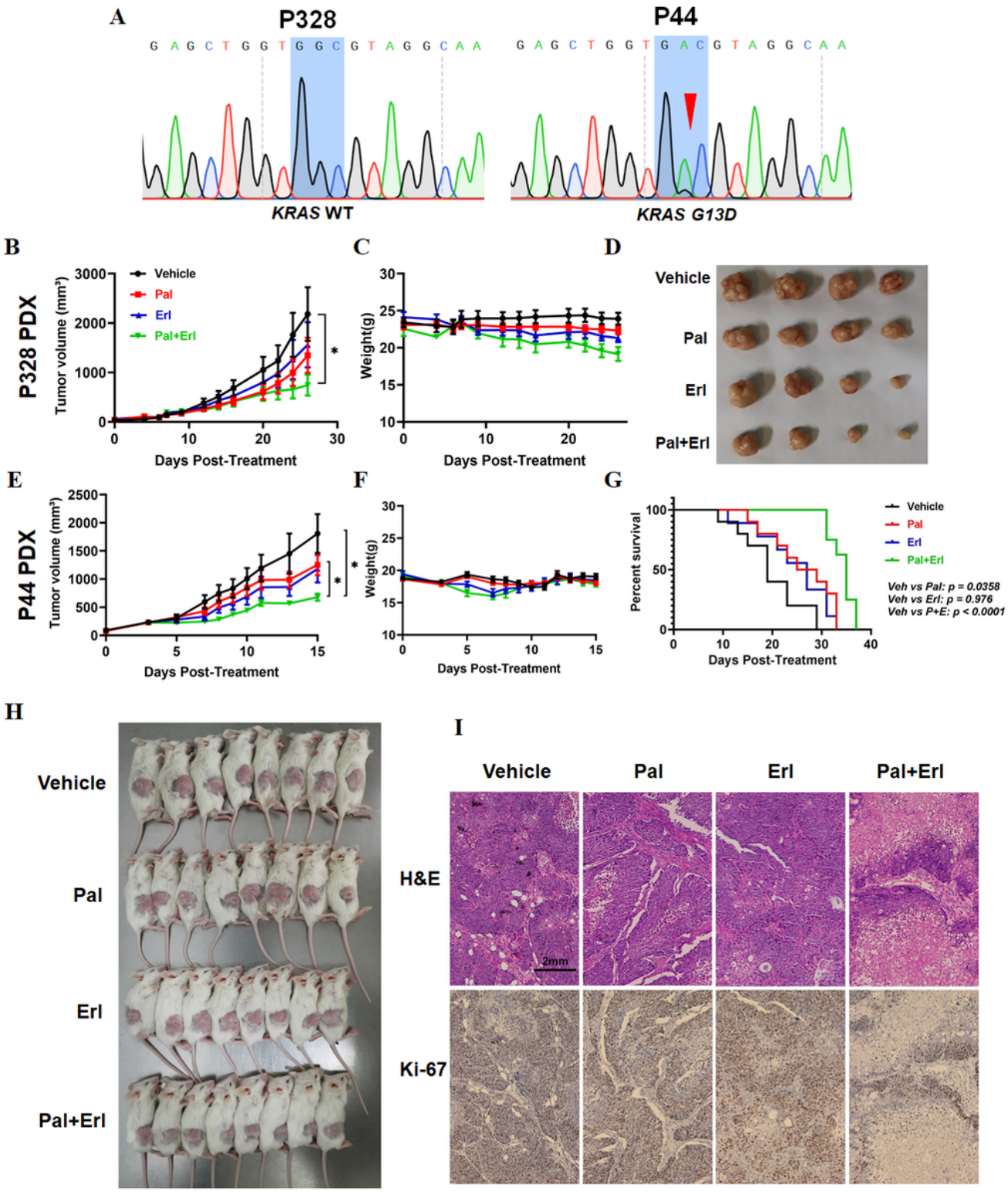

Figure 6

Evaluation of the efficacy of PE-combination in CRC PDX models. (a) DNA sequences of the c.38 loci in KRAS genes of P328 and P44 CRC specimen. (b-d) The curves of PDX tumor volumes (b), body weights (c) and four representative tumor samples isolated from each treatment group (d) of NCG mice carried P328 PDX upon treatment of palbociclib and/or erlotinib. (e–g) The curves of PDX tumor volumes (e), body weights (f), Kaplan-Meier survival curves (g), eight representative P44 PDX bearing mice in each

treatment group (h), and tumor tissue stained with H&E or Ki-67 (i) of NCG mice upon treatment of palbociclib and/or erlotinib. Scale bar, 2 mm.